Structure design and rice threshing performance of the variable-speed inertial pulley for simulating artificial threshing

Tiantian Jing[1], Zhong Tang[1,2], Shuaihua Hao[1,3], Cheng Shen[4*], Ting Wang[5], Meilin Wang[1]

(1. *School of Agricultural Engineering, Jiangsu University, Zhenjiang 212013, Jiangsu, China*;
2. *Key Laboratory of Intelligent Equipment and Robotics for Agriculture of Zhejiang Province, Hangzhou 310058, China*;
3. *College of Engineering, China Agricultural University, Beijing 100083, China*;
4. *Nanjing Institute of Agricultural Mechanization, Ministry of Agriculture and Rural Affairs, Nanjing 210014, China*;
5. *Jiangsu World Agriculture Machinery Co., Ltd (WORLD A/M), Zhenjiang 212311, Jiangsu, China*)

Abstract: Due to the small models and compact structures, small harvesters have also caused problems such as poor threshing separation performance and large loss rates. In order to solve unstable cleaning effects of small harvesters when they facing different working conditions, this study selected rice plants in hilly areas for the experiment. Tensile breaking force of different parts of mature rice was tested, which revealed the fracture mechanism of each part under the combined force. Inertial threshing method was used to simulate artificial plate bin and design three kinds of non-circular pulley variable speed transmission threshing mechanism. With the help of transient inertia force, threshing force was compensated. This paper tested the harvesting performance of the variable speed threshing device with the help of the harvest performance test. Results show when facing the small rice planting area, the T/2 variable speed threshing device has better cleaning performance, and also the harvest loss rate of T/4 variable speed threshing device is the lowest. Compared with the constant speed threshing device, the impurity content rate of the variable speed threshing device is increased by 0.64% to 8.76%; the loss rate is reduced by 0.45% to 1.79%, which provides a basis for the optimization design of small combine harvester in hilly areas.

Keywords: small harvesters, fracture mechanism, transient inertia force, non-circular pulley
DOI: 10.25165/j.ijabe.20241701.8325

Citation: Jing T T, Tang Z, Hao S H, Shen C, Wang T, Wang M L. Structure design and rice threshing performance of the variable-speed inertial pulley for simulating artificial threshing. Int J Agric & Biol Eng, 2024; 17(1): 33–40.

1 Introduction

Rice is an important food crop. The yield of rice plays an important role in regional development[1-3]. At present, mature rice is mainly harvested mechanized by combine harvesters[4,5], in hilly areas, small harvesters are used for harvesting. However, when facing different landforms and types of rice, the working state of small harvester has unstable factors[6]. Mechanical characteristics of rice stem are affected by variety, climate and season[7], complex stress state and serious fracture state in the process of threshing will lead to difficulties in late selection. At the same time, rice grain breakage, entrainment loss and non-depuration loss caused will cause serious grain loss in the harvesting process of rice. Therefore, design an efficient threshing device based on the mechanical characteristics of rice is significant for ensuring rice harvest.

The mechanical properties of rice are multidirectional. Kruszelnicka et al.[8] studied the mechanical properties of grain and analyzed its influence on processing characteristics. The physical characteristics of rice grains and stems are substantially affected during harvest by the field environment and harvest time[9]. During the threshing process, the grain may be subjected to loads such as extrusion and bending[10-12]. In the process of rice threshing, the study of its mechanical properties can analyze the effect of load on the grain breakage rate during threshing. Studies on the mechanical properties of rice leaves (sheath, leaf and ring) can provide a basis for cleaning work[13,14]. The connection between grain and stalk can measure the difficulty of threshing, further reduce the number of stalks in the threshing process, and improve the threshing effect.

However, the mechanical properties of rice directly affect its threshing quality, and rice will be subjected to various forces such as gravity and collision during threshing[15,16]. However, due to compact structure and short threshing time of small combine harvesters, problems such as easy winding of stems and leaves and serious breakage of rice leaves often occur in the threshing process[17], resulting in axial pulsation impact and rolling imbalance[18,19]. It also affects the loss rate and damage rate of grain[20]. At present, the common threshing device with constant transmission ratio has a high loss rate at harvest for rice under different planting conditions. Many scholars propose to improve the threshing effect by improving the clearance, rotation speed, or diameter of the threshing cylinder[21-23]. However, it is not suitable for complex operating environment in hilly area. Tian et al.[24,25] designed a differential threshing device to adjust the differential speed between a single drum and a multistage drum, which improves the effect of rice threshing.

The existing research cannot propose a better threshing method based on the fracture mechanical properties of rice. This study tests

Received date: 2022-12-05 **Accepted date:** 2023-11-01
Biographies: **Tiantian Jing**, Postgraduate, research interest: intelligent harvesting machinery, Email: 3143231562@qq.com; **Zhong Tang**, Professor, research interest: agricultural mechanization engineering, Email: zht@ujs.edu.cn; **Shuaihua Hao**, Postgraduate, research interest: intelligent harvesting machinery, Email: 2082619648@qq.com; **Ting Wang**, Engineer, research interest: intelligent harvesting machinery, Email: 15996802195@163.com; **Meilin Wang**, Postgraduate, research interest: intelligent harvesting machinery, Email: 1131462006@qq.com.
***Corresponding author: Cheng Shen**, Assistant Professor, research interest: agricultural mechanization engineering. Nanjing Institute of Agricultural Mechanization, Ministry of Agriculture and Rural Affairs, No.100 Liuying, Xuanwu District, Nanjing 210014, China. Tel: +86-25-84346078, Email: shencheng@caas.cn.

the mechanical properties of mature rice plants, and reveals the mechanism of fracture failure of rice stem subjected to combining force. Based on the cross-axial flow threshing device test bench, three kinds of non-circular pulley transmission mechanisms are designed to realize the variable speed inertial threshing method for simulating the artificial threshing of plate bin. In order to solve the problem that the influence law of the change of feeding amount on the threshing and separation performance is unclear in the process of threshing, the threshing and separation performance test under different feeding amount are carried out, and the threshing and separation performance of rice threshing device with different feeding amount is obtained.

2 Materials and methods

2.1 Tensile composite fracture mechanics test of rice components

To determine the threshing force of mature rice grains in hilly areas, in this study, "Huiliangyou silk seedling rice" from Zhenjiang City of China was used as the experimental material to study the threshing and separation performance. Its structure is shown in Figure 1a. This study selected well-grown, the mechanical characteristics of mature rice plants without obvious damage to the stem surface. Field planted experimental rice rows were 150 mm apart.

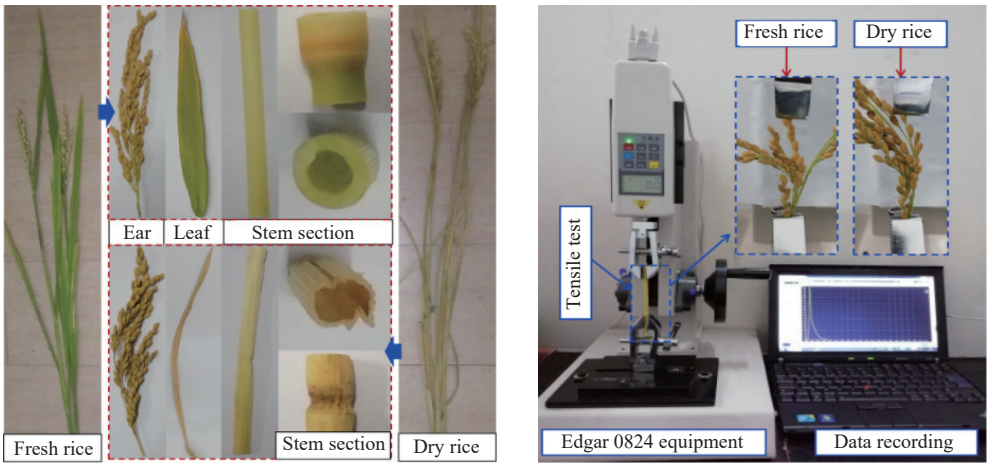

a. Classification and treatment of rice samples b. Push pull tester test equipment

Figure 1 Test apparatus for rice sample classification and tensile property test

The threshing process of rice in the threshing roller can be approximated to the fracture under 2-point tension. Due to the different physical properties of the stalks in different states, in this study, the tensile properties of various parts of rice were tested in their natural and dry states using Edgar 0824 push-pull testing machine. The test procedure is shown in Figure 1b.

After completing the 2-point tensile performance test of each part of the rice sample, the statistical analysis of its breaking force is shown in Figure 2. As shown in Figure 2b, the breaking force of the stalk is significantly smaller than that of the other parts, and the maximum threshing force of the stalk is only 1.7 N. The index that is only smaller than the threshing force of the stalk is the breaking force of the upper part of the leaf. It can be seen that in the process of threshing, the rotational force of the threshing cylinder must be greater than 1.7 N and less than 6.9 N to achieve better threshing work.

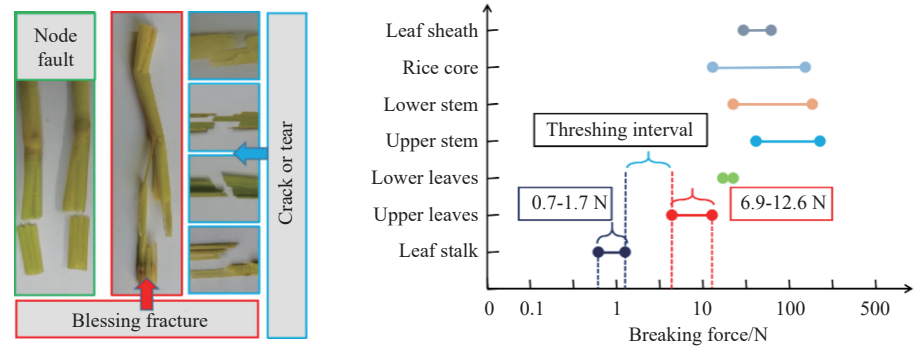

a. Fracture form in various parts of rice b. Tensile breaking force of each part of rice

Figure 2 Fracture form and fracture force analysis of rice samples

2.2 Design of transmission pulley with transient inertia force compensation

At present, all threshing devices adopt circular pulleys for power transmission, so the speed of threshing cylinder is constant, which cause the threshing effect is general. Rice threshing in artificial board barn is rarely causes stem and rice leaf to break. The key reasons are as follows: 1) the tensile breaking force of rice stalk is different from that of stem and rice leaf and is the minimum point; 2) the stem, rice leaf and rice stalk are subjected to large transient inertial force when rice is manually thrown into the bannel.

Therefore, in order to achieve good threshing effect, this paper designs a variable speed transmission device to make the rice grain break at the point of the minimum tensile breaking force with the help of transient inertia force. In order to imitate the artificial threshing, the transmission structure of the threshing device is designed as a non-circular pulley transmission mechanism to realize

the variable speed rotation of the threshing cylinder, and the inertia force generated by the variable speed is used to simulate the artificial threshing method for rice threshing.

In this study, the range of rotational angular acceleration was determined by using the range of threshing force of rice, and the equation about the short axis of non-circular pulley was obtained. For the non-uniform rigid body, the compound pendulum method can be used to solve the moment of inertia, the non-circular pulley designed in this study has symmetry, and its moment of inertia J can be obtained according to Equation (1).

$$J = \frac{mgR_0T^2}{4\pi^2} \tag{1}$$

where, m is the mass of the non-circular pulley, kg; g is the constant acceleration of gravity, 9.8 m/s^2, R_0 is the semi-major axis of the non-circular pulley, 114 mm; T is the suspension swing period of the non-circular pulley, s;

The size and weight of the non-circular pulley designed in this paper is approximately the same as the circular pulley with radius R_0. According to Figure 1, to achieve good threshing effect, threshing force must be greater than 1.7 N and less than 6.9 N. Therefore, Equation (2) can be obtained.

$$\begin{cases} M = FR_1 \\ 1.7\ \text{N} < F < 6.9\ \text{N} \end{cases} \tag{2}$$

where, F is threshing force, N; R_1 is the outer diameter of the threshing cylinder, here it is 0.32 m.

The threshing cylinder is generally driven by circular chain/pulley. Its rotational speed is generally 600-800 r/min, in this paper, rotational speed is 600 r/min. The motor speed of the test bench for the cross-axial flow threshing cylinder device is 2800 r/min. For the driving pulley and non-circular pulley, the rotational linear velocity is the same, for the threshing cylinder and non-circular pulley, the rotational angular velocity is the same. Therefore, after determining the angular velocity of threshing cylinder, the short half axis of the non-circular pulley is 105.8445-106.5501 mm, and 106 mm is taken in this study.

The belt, small pulley and non-circular pulley constitute the whole variable speed transmission mechanism. The polar coordinate system was established with the rotation center of each pulley as the pole and the counterclockwise direction as the positive direction. In the coordinate system O_{xy}, the polar equation of the tangent line of the curve is expressed as $p=p(\theta)$, as shown in Figure 3.

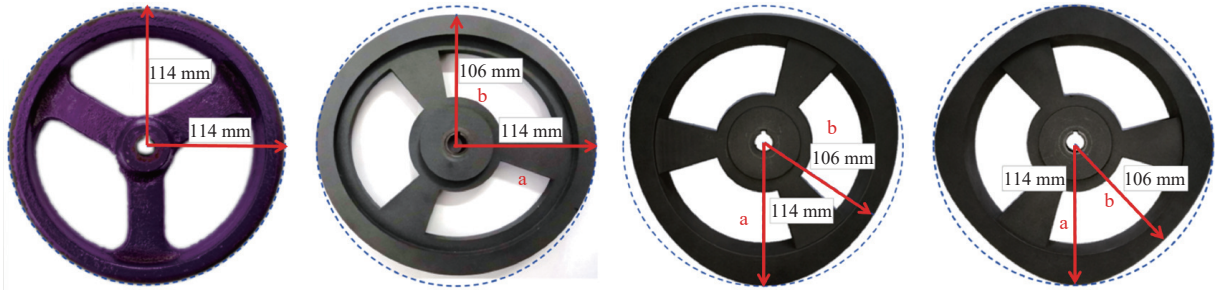

a. Pulley 1 b. Pulley 2 c. Pulley 3 d. Pulley 4

Note: a and b in b., c., and d. are the long half axis and short half axis, respectively.

Figure 3 Non-circular pulley structure model

The designed non-circular pulley has the same shaft length; the radius change period is different within 360°. Taking 360° of the circular pulley as a period T of radius change, then the change period of radius of pulley 2, 3 and 4 is T/2, T/3, T/4, respectively. The nodal curve equation of the designed non-circular pulley in a change period is obtained by MATLAB fitting, as shown in Equations (3)-(6).

$$p_1 = 114 \tag{3}$$

$$p_2 = -1.499\times10^{-7}\theta_2^4 + 5.408\times10^{-5}\theta_2^3 - 0.005\,142\theta_2^2 + 0.047\,73\theta_2 + 113.9\ (0^\circ \le \theta_2 \le 180^\circ) \tag{4}$$

$$p_3 = -7.259\times10^{-7}\theta_3^4 + 1.742\times10^{-4}\theta_3^3 - 0.010\,92\theta_3^2 + 0.056\,43\theta_3 + 113.9\ (0^\circ \le \theta_3 \le 120^\circ) \tag{5}$$

$$p_4 = -2.695\times10^{-6}\theta_4^4 + 4.854\times10^{-4}\theta_4^3 - 0.023\,74\theta_4^2 + 0.1692\theta_4 + 113.7\ (0^\circ \le \theta_4 \le 90^\circ) \tag{6}$$

For the angular velocity of threshing cylinder, the transmission equation can be established according to the outer contour parameters. In this study, MATLAB was used to fit the angular velocity of a non-circular pulley as a function of rotation time and angular velocity, as shown in Equations (7)-(9).

$$\omega_2 = -1.142\times10^9 t_2^4 + 1.334\times10^8 t_2^3 - 4.261\times10^6 t_2^2 + 3.104\times10^4 t_2 + 4452(0 \le t_2 \le 0.0421) \tag{7}$$

$$\omega_3 = 6.806\times10^9 t_3^4 - 2.986\times10^8 t_3^3 + 1.806\times10^6 t_3^2 + 3.553\times10^4 t_3 + 4186(0 \le t_3 \le 0.0288) \tag{8}$$

$$\omega_4 = -2.472\times10^9 t_4^4 - 3.252\times10^8 t_4^3 + 1.13\times10^7 t_4^2 - 7.775\times10^4 t_4 + 4344(0 \le t_4 \le 0.0208) \tag{9}$$

Pulley 3 rotates for about 0.0863 s for a cycle of 120°. The pulley 4 rotates for about 0.0831 s for a cycle of 90°. The angular velocity of threshing cylinder can be obtained by taking the derivative of Equations (7)-(9).

Let the rotation angle of pulley 1 be φ_1, and the corresponding rotation angle of pulley 2 be φ_2. The center distance is z, mm. The tangent points of belt and two pulleys pitch curves are C_1 and C_2, and the pitch curve parameters of these two points are p_1, θ_1 and p_2, θ_2 respectively. When s_1 is used to represent arc length $C_{10}C_1$ and s_2 is used to represent arc length $C_{20}C_2$, then the length between C_1C_2 should be $T_{-s_1+s_2}$, thus conditional Equation (10) is available.

$$T_{-s_1+s_2} = p_1(\theta_1) + z\sin(\theta_1+\varphi_1) - p_2(\theta_2) \tag{10}$$

where, s_1 and s_2 are satisfied:

$$\begin{cases} s_1 = \int_{\theta_0}^{\theta_1} \left(p_1 + p_1''\right) \mathrm{d}\theta_1 \\ s_2 = \int_{\theta_0}^{\theta_2} \left(p_2 + p_2''\right) \mathrm{d}\theta_2 \end{cases} \tag{11}$$

It is obtained by substituting it into Equation (10).

$$T=\int_{\theta_0}^{\theta_1}\left(p_1+p_1''\right)d\theta_1-\int_{\theta_0}^{\theta_2}\left(p_2+p_2''\right)d\theta_2+\dot{p}_1(\theta_1)+ z\sin(\theta_1+\varphi_1)-\dot{p}_2(\theta_2) \quad (12)$$

Meanwhile, Equation (13) and (14) can be obtained.

$$\varphi_1+\theta_1=\varphi_2+\theta_2 \quad (13)$$

$$p_2-p_1=-z\cos(\varphi_1+\theta_1) \quad (14)$$

It can be seen that the tangent polar equations of the small pulley and the two-section curve of the pulley are Equations (14) and (4). Then, according to Equation (9), the transmission ratio i_{02} of the variable speed transmission mechanism composed of small pulley and pulley 2 can be expressed as Equation (15).

$$i_{02}=\frac{p_2}{p_0}=-5.2596\times10^{-9}\theta_2^4+1.8975\times10^{-6}\theta_2^3-1.8042\times10^{-4}\theta_2^2+ 1.6747\times10^{-3}\theta_2+3.9965(0^\circ\le\theta_2\le180^\circ) \quad (15)$$

Given the value of θ_2, other motion parameters of the transmission mechanism can be calculated according to the equation. Similarly, the instantaneous change curve of transmission ratio of variable speed transmission mechanism composed of pulley 0, pulley 3 and pulley 4 can be calculated. The relationship between transmission ratio i and pulley angle φ is obtained as listed in Table 1.

Table 1 Parameters of non-circular pulley drive

θ_2/(°)	φ_2/(°)	i_{02}	θ_3/(°)	φ_3/(°)	i_{03}	θ_4/(°)	φ_4/(°)	i_{04}
0	111.7961	3.9965	0	111.7961	3.9965	0	111.7424	3.9895
30	81.2987	3.9313	30	80.7216	3.8555	30	80.3100	3.8012
60	50.2193	3.7892	60	49.7427	3.7261	60	50.3032	3.8003
90	19.7273	3.7240	90	20.7248	3.8559	90	21.7348	3.9885
120	–9.7917	3.7877	120	–8.1989	3.9971			

The transmission structure of the device consists of a small belt, a large belt, and a V-belt. This paper selects the V-belt for transmission. The non-round contour structure is shown in Figure 4, and its pulley groove is drawn according to the A-type V-belt structure. Model A ordinary V-belt section is 11 mm width, top width of 13 mm, 8 mm height, and wedge angle 40°. Since the designed belt parts are non-standard parts, this article selects 3D printed processing methods for processing of 3 parts. The material attribute of the parts is listed in Table 2.

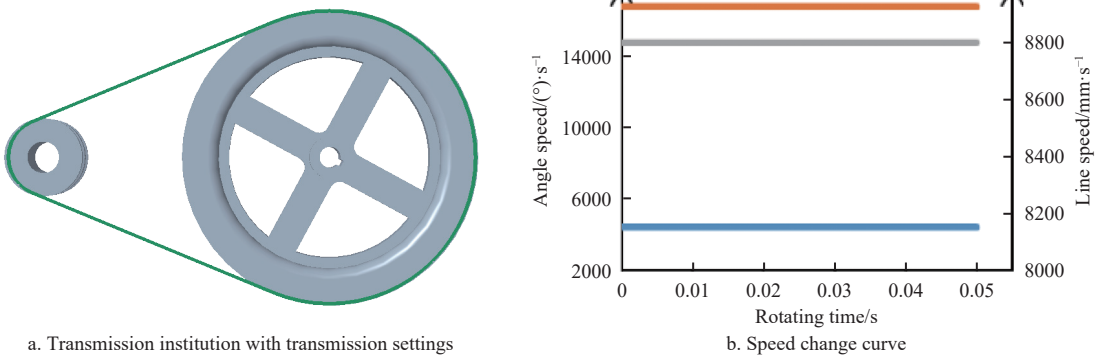

a. Transmission institution with transmission settings b. Speed change curve

Figure 4 Circle Band pulley transmission mechanism simulation

Table 2 3D printing material attribute

θ_2/(°)	φ_2/(°)	i_{02}	θ_3/(°)	φ_3/(°)	i_{03}	θ_4/(°)	φ_4/(°)	i_{04}
0	111.7961	3.9965	0	111.7961	3.9965	0	111.7424	3.9895
30	81.2987	3.9313	30	80.7216	3.8555	30	80.3100	3.8012
60	50.2193	3.7892	60	49.7427	3.7261	60	50.3032	3.8003
90	19.7273	3.7240	90	20.7248	3.8559	90	21.7348	3.9885
120	–9.7917	3.7877	120	–8.1989	3.9971			

The processing pulleys after processing has a high strength, which can be installed and meets the normal operation of the decarling device. This article performs institutional motion simulation and analysis in Creo Parametric 5.0 software. When assembly, use mechanical constraints to connect the component and then enter the mechanism module to perform motion simulation and basic motion analysis.

It can be seen from Figure 4 that the pulley 0 angle speed is 16 800°/s, which is 293.2153 rad/s. The speed of pulley 1 angle of the pulley is 4421.05°/s, which is 77.1619 rad/s. The pulley 1 is consistent with the speed of the 0 line of the pulley, 8796.46 mm/s. The angle speed and line speed of the transmission mechanism consisting of pulley 0 and the pulley 1 will not change. The transmission mechanism composed of a pulley 0 and a pulley 1 can enable the decarcular roller to rotate constant speed. The angular and linear velocities of the three non-circular pulleys were simulated, and the results are shown in Figure 5.

It can be seen from Figure 5a that the changing speed of the rotating angle of the pulley 2 is consistent with the angle speed changes entered in the Creo software. The speed of the pulley and the line speed of the line is periodic, and the rotation of the pulley is 180° to one cycle. The range of 2 angle speed of the pulley is 4199.109°/s-4511.241°/s, that is, 73.2883-78.7360 rad/s. The speed change range on the long axis of the pulley 2 is 8359.374-9090.943 mm/s.

It can be seen from Figure 5b that the change of the rotating angle speed of the pulley 3 and the rotation 4 is basically the same as the angle speed changes entered in the Creo software. Rotate 3 rotation for 120° for one cycle, which is about 0.288 s. Rotate 4 rotation at 90° to one cycle, which takes about 0.0208 s. The range of 3 angle speed of the pulley is (4192.6211-4497.5724)°/s, which is 73.1750-78.4974 rad/s. The range of the speed of the 3 line of the pulley is 8323.2716-8928.6669 mm/s. The range of 4 angle speed of the pulley is (4192.3544-4498.7758)°/s, which is 73.1704-78.5185 rad/s. The range of the 4-line speed of the pulley is 8304.8389-8911.8441 mm/s.

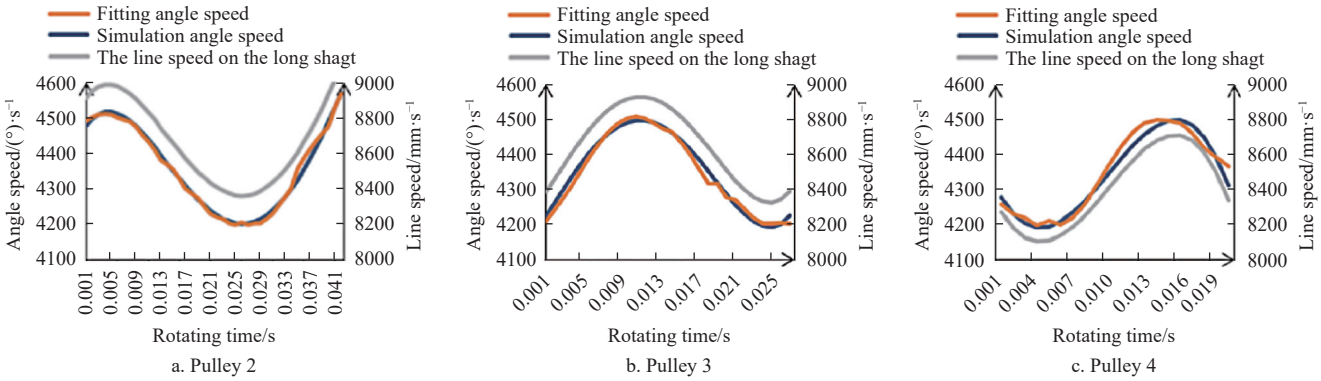

Figure 5 Bringing pulley angle speed, line speed change curve

2.3 Harvest performance test of variable speed pulley

In order to verify the working performance of the designed non-circular pulley, in this study, the impurity content rate and loss rate were tested under different grain harvest. The transmission device and structural model of threshing cylinder of combine harvester is shown in Figure 6. In order to ensure the threshing effect, the speed is generally 600-800 r/min, the test bench selects the rotational speed 600 r/min.

Field mature rice from Zhenjiang City, Jiangsu province was used in the experiment, and there was no significant difference in physical and mechanical properties between the rice variety and the rice variety from hilly areas. The threshing performance of the threshing device was tested by manually feeding five groups of rice samples of the same weight continuously. The experimental rice samples are shown in Figure 7. From the first group of rice samples enter the threshing chamber to the last group of rice samples enter the threshing chamber can be approximated as threshing cylinder feeding weight is 0.5, 1.0, 1.5, 2.0, 2.5 kg/s. After threshing, the exhaled materials were collected from the bottom of the concave plate screen of the threshing device and the outlet of the grass for subsequent test and analysis. The weight of residue and grain after manual cleaning was measured by electronic scale and recorded. The stem in the mixture under the concave plate sieve was selected manually for subsequent test and analysis. The test process is also shown in Figure 7.

The belt model A838 is still used during the installation of non-round pulleys. Irregular shape of pulley will lead to belt relaxation, affecting the working ability of belt drive. The test bench of the threshing device is small and compact in structure. Therefore, according to the structure of the threshing device, the tension of the pulley was finally selected by adjusting the center distance. The installation mode of variable speed transmission mechanism is shown in Figure 8.

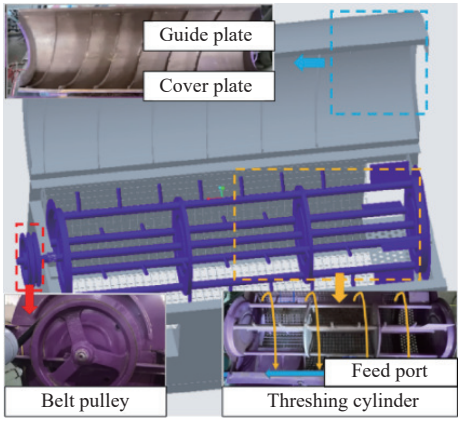

Figure 6 Structure promotion and transmission mode of threshing device

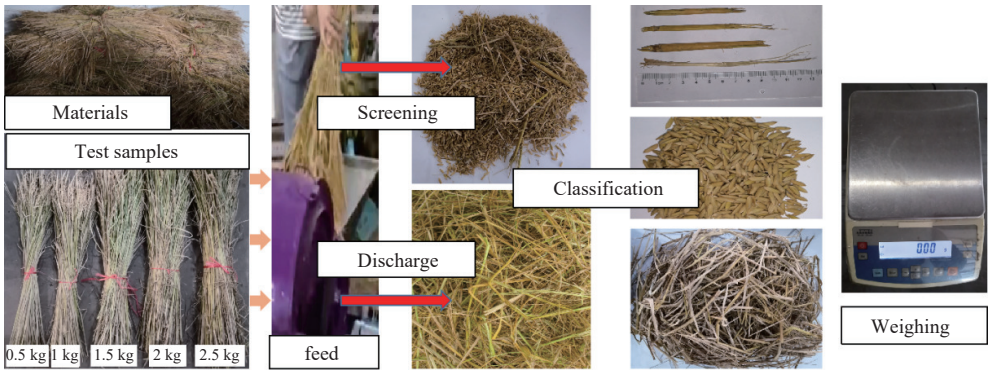

Figure 7 Schematic diagram of threshing performance test process

Figure 8 Installation mode of variable speed transmission mechanism

In this experiment, three indexes were designed to evaluate the threshing performance, which were the rate of impurity and the rate of loss and the degree of stem destruction. Impurity content refers to the percentage of the impurities discharged from the lower concave plate by the threshing device in the total mass of the mixture, including non-grain substances such as straw, glume, stone and so on. The impurity rate can be calculated by Equation (16).

$$Z_Z = \frac{m_2}{M_2} \times 100\% \quad (16)$$

where, Z_Z is the impurity content rate; m_2 is the impurity mass output by the threshing device from the lower concave plate, kg; M_2 is the total mass of the mixture output by the threshing device from the lower concave plate, kg.

The loss rate of the threshing device is the percentage of the lost grain mass to the receivable grain mass. The loss rate includes entrainment loss rate and unstripped net loss rate. The loss rate can be calculated by Equation (17).

$$S = \frac{m_3}{M_3} \times 100\% \quad (17)$$

where, S is the loss rate; m_3 is the weight of grain entrainment and undepurated by threshing device, kg; M_3 is the grain weight receivable by the threshing device, kg.

The degree of stalk destruction was evaluated in terms of the length of the rice stalks in the mixture under the gravure screen, and the broken stalks were categorized into long, medium and short stalks. Stem length above 200 mm is long stalk, between 70-200 mm is middle stalk, and below 70 mm is short stalk. The proportion of stalks with different lengths in the extruder mixture under gravure sieve was counted.

3 Results and discussion

3.1 Work performance analysis and test of threshing cylinder

In order to solve the problem of the error of the test data, the total mixture under the concave screen and the weight of the clear grain were used as the benchmark to calculate other data in the processing of the test. The analysis of threshing performance test results is shown in the Figure 9. It shows the proportion of the weight of each part under different test conditions and the number of relatively intact stems still retained in the mixture under the concave plate and sieve.

The threshing test results of the threshing cylinder with fixed speed are shown in Figure 9a. Under different threshing conditions, about 2.09%-7.34% of the impurities (the impurity content rate was 2.09%-7.34%) and 92.66%-97.91% of the grains, and the rest of the mixture was discharged from the weed outlet. The threshing test results of *T*/2 variable speed threshing cylinder is shown in Figure 9b. Under different threshing conditions, about 2.73%-9.93% of the impurities (2.73%-9.93% of the impurities) and 90.07%-97.27% of the grains, and the remaining mixture, accounting for 44.39%-63.13% of the total mass, were discharged from the weed removal port. Compared with threshing cylinder with fixed speed, the *T*/2 variable speed threshing cylinder showed low impurity content at 0.5 kg/s.

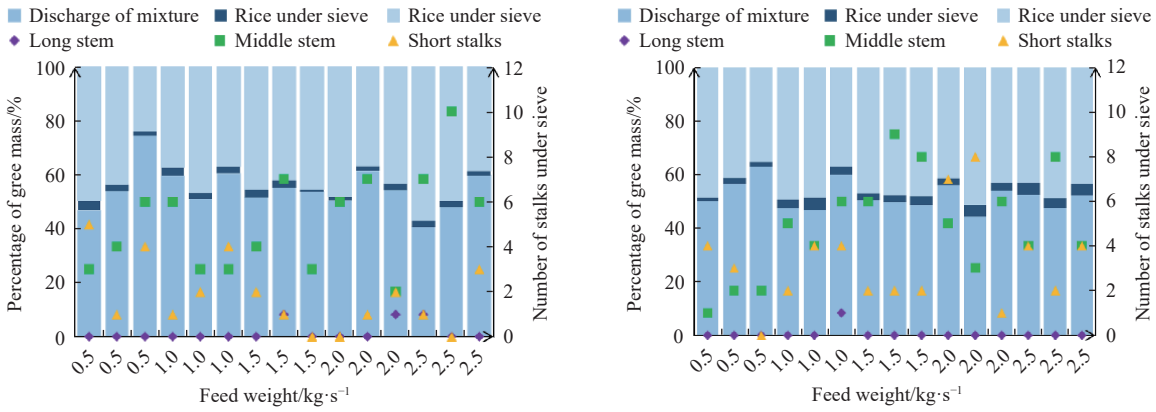

a. Threshing cylinder with fixed speed

b. *T*/2 variable speed threshing roller

Figure 9 Percentage of shedding mass and number of stem roots in the shedding mixture under a fixed speed threshing sieve

In the threshing test of *T*/3 variable speed threshing cylinder, the threshing cylinder was blocked when 2 kg rice was fed, and the test data could not be obtained. The test results are shown in Figure 10a. Only three different feeding conditions were tested, the grain containing impurity rate was 6.59%-12.79% and 87.21%-93.41%. In the whole process of the threshing test, the length of the stem dropped from the concave plate screen was less than 200 mm, but its impurity content rate was still higher than that of the constant speed threshing cylinder. From the point of view of impurity content, the *T*/3 variable speed threshing cylinder has the problems of low threshing feed rate and high threshing impurity content. The test results of *T*/4 variable speed threshing cylinder are shown in Figure 10b. Under different threshing conditions, about 6.60%-16.10% of the impurities (the impurity content rate is 6.60%-16.10%) and 83.90%-93.4% of the grains. The rest of the mixture, about 39.67%-57.2% of the total mass, is discharged from the weed outlet. The impurity content rate of *T*/4 variable speed threshing cylinder is slightly higher than that of constant speed threshing cylinder.

In conclusion, the *T*/2 variable speed threshing drum showed better threshing performance at 0.5 kg/s in terms of the level of impurity content of the discharged material. Under other feeding conditions, the constant speed threshing cylinder shows better threshing performance. From the point of view of feeding quantity, the constant speed threshing cylinder, *T*/2 speed threshing cylinder and *T*/4 speed threshing cylinder are better than the *T*/3 speed threshing cylinder.

3.2 Loss rate analysis of threshing device

High moisture content of rice, low speed of threshing cylinder, large clearance of concave plate and sieve, large feeding rate, all of them may lead to large threshing loss. Calculate the loss rate of threshing device under different transmission modes, including entrainment loss and non-stripping net loss. The loss rate results of threshing device under different transmission modes and different feeding quantities are shown in Figure 11.

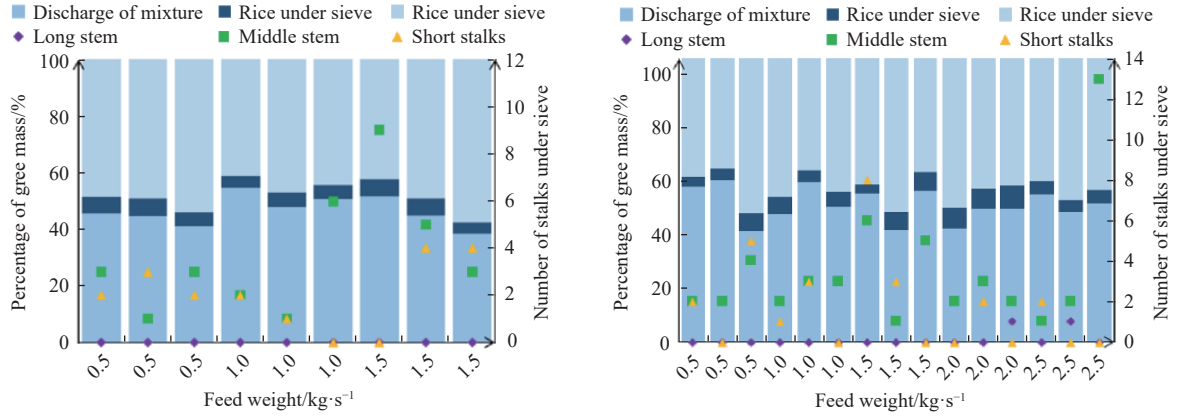

a. *T*/3 variable speed threshing roller b. *T*/4 variable speed threshing roller

Figure 10 Percentage of shedding mass and number of stem roots in the shedding mixture under a variable speed threshing sieve

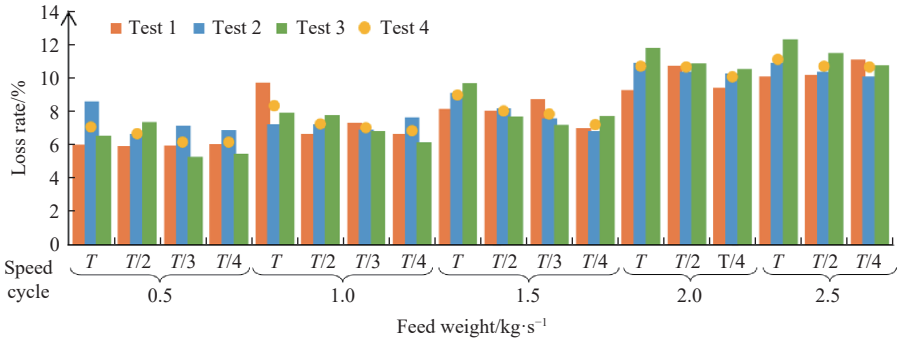

Figure 11 Loss rates of threshing units under different operating conditions

As shown in Figure 11, the loss rate of threshing cylinders with constant and variable speed was in the range of 6.13%-11.11%. With the increase of feeding rate, the loss rate of threshing device increases slightly. It may be that the thickness of the material layer entering the threshing cylinder becomes larger when the feeding amount increases, which reduces the probability of grain passing through the material layer and leads to the increase of entrainment loss rate. Under the same feeding conditions, the loss rate of the variable speed threshing cylinder was slightly lower than that of the constant speed threshing cylinder. Compared with the fixed speed threshing cylinder, the designed variable speed threshing cylinder can reduce the loss rate of 0.45%-1.79% and improve the threshing and separation performance.

4 Conclusions

1) Tensile properties of each part of rice under natural state and dry state was tested, which shown that the fracture position of each part was not fixed, and the maximum breaking force of grain was 1.7 N. Therefore, the hitting force of the nail teeth must be greater than 1.7 N and less than 6.9 N to achieve good threshing function.

2) A transient inertia compensation threshing method was proposed to simulate the threshing of rice grains in an artificial plate bin. Three non-circular pulleys were designed according to the range of threshing force of paddy grain, and the transient transmission ratio of the variable speed drive mechanism was deduced to be periodically changing in the range of 3.7240-4.0000.

3) The threshing performance test of the variable speed threshing drum was carried out on the test bed of the transverse axial flow threshing device. The variable speed threshing drum was analysed from the point of view of impurity content and loss rate and it was found that the variable speed threshing drum was able to exhibit better threshing and separation performance to a certain extent.

Acknowledgements

This research work was financially supported by the National Natural Science Foundation of China (Grant No. 52175235), Key Laboratory of Intelligent Equipment and Robotics for Agriculture of Zhejiang Province (Grant No. 2023ZJZD2302), Jiangsu Province and Education Ministry Co-sponsored Synergistic Innovation Center of Modern Agricultural Equipment (Grant No. XTCX2007), and Taizhou Science and Technology Support Plan (Agriculture) Project (TN202219).

[References]

[1] Cordero-Lara K I. Temperate japonica rice (*Oryza sativa* L.) breeding: history, present and future challenges. Chilean Journal of Agricultural Research, 2020; 80(2): 303–314.

[2] Dale D S, Liang L, Zhong L H, Reba M L, Runkle B R K. Deep learning solutions for mapping contour levee rice production systems from very high resolution imagery. Computers and Electronics in Agriculture, 2023; 211: 107954.

[3] Dhillon A K, Sharma N, Dosanjh N K, Goyal M, Mahajan G. Variation in the nutritional quality of rice straw and grain in response to different nitrogen levels. Journal of Plant Nutrition, 2018; 41(15): 1946–1956.

[4] Tang Z, Zhang H, Wang X Z, Gu X Y, Zhang B, Liu, S F. Rice threshing state prediction of threshing cylinder undergoing unbalanced harmonic response. Computers and Electronics in Agriculture, 2023; 204: 107547.

[5] MOA (Ministry of Agriculture, China). Annual rice production in China.https://data.stats.gov.cn/easyquery.htm?cn=C01 Accessed on [2020-04-05].

[6] Lu S, Cheng G, Li T, Xue L, Liu X J, Huang J Z, et al. Quantifying supply chain food loss in China with primary data: a large-scale, field-survey based analysis for staple food, vegetables, and fruits. Resources, Conservation and Recycling, 2022; 177: 106006.

[7] Huang J L, Liu W Y, Zhou F, Peng Y J. Effect of multiscale structural parameters on the mechanical properties of rice stems. Journal of the Mechanical Behavior of Biomedical Materials, 2018; 82: 239–247.

[8] Kruszelnicka W, Marczuk A, Kasner R, Baldowska-Witos P, Piotrowska

K, Flizikowski J, et al. Mechanical and processing properties of rice grains. Sustainability, 2020; 12(2): 552.

[9] Ma Z, Zhu Y L, Chen S R, Traore S N, Li Y M, Xu L Z, et al. Field investigation of the static friction characteristics of high yielding rice during harvest. Agriculture, 2022; 12(3): 327.

[10] Zhou F, Huang J L, Liu W Y, Deng T, Jia Z K. Multiscale simulation of elastic modulus of rice stem. Biosystems Engineering, 2019; 187: 96–113.

[11] Du Z, Hu Y, Buttar N A. Analysis of mechanical properties for tea stem using grey relational analysis coupled with multiple linear regression. Scientia Horticulturae, 2020; 260: 108886.

[12] Xue K, Gao K J, Wang T J, Zhang X S, Zhang S, Kuang F M, etal. Biomechanical modeling of rice seedling stalk based on multi-scale structure and heterogeneous materials. Computers and Electronics in Agriculture, 2023; 210: 107904.

[13] Chang T G, Zhao H L, Wang N, Song Q F, Xiao Y, Qu M N, et al. A three-dimensional canopy photosynthesis model in rice with a complete description of the canopy architecture, leaf physiology, and mechanical properties. Journal of Experimental Botany, 2019; 70(9): 2479–2490.

[14] Chao S, Mitchell J, Prakash S, Bhandari B, Fukai S. Effects of variety, early harvest, and germination on pasting properties and cooked grain texture of brown rice. Journal of Texture Studies, 2022; 53(4): 503–516.

[15] Tang Z, Zhang B, Wang B, Wang M L, Chen H, Li Y M. Breaking paths of rice stalks during threshing. Biosystems Engineering, 2021; 204: 346–357.

[16] Zhang B, Tang Z, Wang M, Li Y. Breaking behavior of wheat stem undergoing multiple forces combination sequence during threshing process. Journal of Agricultural Science and Technology, 2022; 24(2): 351–363.

[17] Chen Y W, Zheng H B, Wang W Q, Kuang N, Luo Y Y, Zou D, et al. Effect of mowing treatment on the main season whole plant biomass and silage quality and yield in regeneration season of ratooning rice. Journal of Agricultural Science and Technology, 2022; 24(8): 161–171.

[18] Koynov S, Wang Y F, Redere A, Amin P, Emady H N, Muzzio F J, et al. Measurement of the axial dispersion coefficient of powders in a rotating cylinder: Dependence on bulk flow properties. Powder Technology, 2016; 292(5): 298–306.

[19] Tang Z, Wang M L, Zhang H T, Zhou Y P, Li Y. Variation and modal characteristic of tangential threshing cylinder undergoing threshing dynamics. Mathematical Problems in Engineering, 2020; 1723893.

[20] Wang Q, Mao H, Li Q. Modelling and simulation of the grain threshing process based on the discrete element method. Computers and Electronics in Agriculture, 178: 105790.

[21] Liu Y B, Li Y M, Dong Y H, Huang M S, Zhang T, Cheng J H. Development of a variable-diameter threshing cylinder for rice combine harvester using MBD-DEM coupling simulation. Computers and Electronics in Agriculture, 2022; 196: 106859.

[22] Su Z., Ding Z, Tian L Q, Lin X, Wang Z M. Design and performance test of variable diameter threshing cylinder of combine harvester. Food Science & Nutrition, 2021; 9(8): 4322–4334.

[23] Alwan S K, Sharifi A, Aljibouri M A, Taher M A. Effect of threshing machines, rotational speed and grain moisture on corn shelling. Bulgarian Journal of Agricultural Science, 2019; 25(2): 243–255.

[24] Tian L Q, Lin X, Xiong Y S, Ding Z. Design and performance test on segmented‐differential threshing and separating unit for head-feed combine harvester. Food Science& Nutrition, 2021; 9(5): 2531–2540.

[25] Sheychenko V, Anelak M, Kuzmych A, Gritsaka O, Assoc, Dudnikov I, et al. Investigation of the grain separation process in the three-drum threshing-separating device of a combine harvester. Mechanization in Agriculture & Conserving of the Resources, 2018; 64(2): 42–45.